Mem. S.A.It. Vol. 89, 50

Memorie della

Stellar rotation and its importance in the interpretation of stellar populations in MCs

Sylvia Ekström[1], Georges Meynet[1], Cyril Georgy[1], and Anahí Granada[2]

[1] Department of Astronomy, Geneva University, Maillettes 51, 1290 Versoix, Switzerland
e-mail: sylvia.ekstrom@unige.ch
[2] Instituto de Astrofísica La Plata, Avenida Centenario (Paseo del Bosque) S/N, B1900FWA La Plata, Argentina

Abstract. I will review the importance of stellar rotation in particular to interpret star clusters in Magellanic Clouds

Key words. Stars: rotation – Stars: evolution – Galaxies: stellar content

1. Introduction

The effects of rotation have been studied since the work of von Zeipel (1924) and Eddington (1925). The 60s and 70s have seen their inclusion in polytropic or simplified models (Roxburgh et al. 1965; Roxburgh & Strittmatter 1966; Faulkner et al. 1968; Kippenhahn & Thomas 1970; Endal & Sofia 1976). In the 90s they were included in more sophisticated models (Pinsonneault et al. 1989; Deupree 1990; Fliegner & Langer 1994; Chaboyer et al. 1995; Meynet 1996). In the end of the 90s, more or less extended grids of stellar models have appeared, that propose rotating models (Langer et al. 1997; Meynet & Maeder 1997; Siess & Livio 1997; Heger et al. 2000; Heger & Langer 2000).

The inclusion of the effects of rotation has brought a significant improvement in the adequation between models and observations like the surface abundances in He, B, and CNO (Heger & Langer 2000; Meynet & Maeder 2000), the predicted surface velocities in clusters (Meynet & Maeder 2000; Martayan et al. 2006), the blue- to red-supergiants rotation in the SMC (Maeder & Meynet 2001), the variation with metallicity of the Wolf-Rayet populations (Meynet & Maeder 2003, 2005; Vink & de Koter 2005), the rotation rates of pulsars (when a strong core-envelope coupling is considered, Heger et al. 2005), or the various supernovae types and GRB progenitors (Meynet & Maeder 2005; Yoon et al. 2006; Georgy et al. 2009).

Rotation modifies the stellar evolution by two different types of actions. 1) There is a deformation of the stellar surface: the characteristics become dependent on the colatitude considered. This affects the stellar parameters deduced from observation, and induces an anisotropy in the mass lost by the star, as detailed in Sec. 2. 2) Some mixing mechanisms are triggered, transporting chemicals and angular momentum. This induces many deviations to the standard evolution, as detailed in Sect. 3.

2. Surface deformation

Rotation induces a deviation to spherical symmetry, proportional to the rotation rate $\omega = \Omega_{\rm surf}/\Omega_{\rm crit}$, where we use $\Omega_{\rm crit} = \sqrt{\frac{8}{27}\frac{G\,M}{R^3_{\rm pol,crit}}}$. In the frame of the Roche model, the maximal extension of the equatorial radius is $R_{\rm eq,crit} = \frac{3}{2}\,R_{\rm pol,crit}$. An oblateness has been observed by interferometry in the case of the rapidly rotating Achernar (α Eridani) for example, in agreement with the value of 1.5 (Domiciano de Souza et al. 2003; Vinicius et al. 2006; Carciofi et al. 2008).

Because of the deformation, the effective gravity becomes dependent on the rotation rate and the colatitude:

$$\vec{g}_{\rm eff} = \vec{g}_{\rm eff}(\Omega,\theta) = \left(-\frac{G\,M}{r^2} + \Omega^2 r\ \sin^2\theta\right) \cap \boldsymbol{e}_r + \Omega^2 r\ \sin\theta\ \cos\theta\ \boldsymbol{e}_\theta \quad (1)$$

Subsequently, the flux inherits from this $\Omega - \theta$ dependence:

$$\vec{F} = \vec{F}(\Omega,\theta) = -\frac{L}{4\pi\,G\,M^\star}\,\vec{g}_{\rm eff}(\Omega,\theta), \quad (2)$$

where

$$M^\star = M\left(1 - \frac{\Omega^2}{2\pi\,G\,\rho_M}\right). \quad (3)$$

According to the Stefan-Boltzman law, we have $F = \sigma T^4$, so the effective temperature gets also the dependence on Ω and θ:

$$T_{\rm eff} = \left[\frac{L}{4\pi\sigma G M^\star}\,g_{\rm eff}(\Omega,\theta)\right]^{1/4} \quad (4)$$

(von Zeipel 1924).

Espinosa Lara & Rieutord (2011) have proposed a more general expression, valid also in the case of rapid rotation. The latitude dependence of the temperature also has been observed in interferometry for the star Altair (α Aquilae, see Monnier et al. 2007) or the stars Alderamin and Rasalhague (α Ceph and α Oph, see Zhao et al. 2009), with values compatible with the models. The deformation becomes significant only for rapid rotation ($\omega > 0.7$). Above this value, a star observed pole-on will present a higher L and $T_{\rm eff}$ than the same star seen with an average inclination. In contrast, a rapidly-rotating star seen equator-on will appear dimmer and cooler than usual (Georgy et al. 2014). There can be repercussions on the mass and age deduced for the observed star. The mass loss is affected by rotation in two ways. First, it is enhanced thanks to the additional support brought by the centrifugal force. Compared to a non rotating star, the enhancement is

$$\frac{\dot{M}(\Omega)}{\dot{M}(0)} = \left[\frac{(1-\Gamma_{\rm Edd})}{\left(1 - \frac{\Omega^2}{2\pi\,G\rho_m} - \Gamma_{\rm Edd}\right)}\right]^{\frac{1}{\alpha}-1} \quad (5)$$

(Owocki & Gayley 1997; Maeder & Meynet 2000; Petrenz & Puls 2000) (however see the discussion by Müller & Vink 2014). Second, the geometry of the mass flux follows the deformation of the surface:

$$\frac{{\rm d}\dot{M}(\theta)}{{\rm d}\sigma} \sim A(\alpha,k)\left(\frac{L}{4\pi\ G\ M^\star}\right)^{\frac{1}{\alpha}-\frac{1}{8}} \cap \frac{g_{\rm eff}^{1-\frac{1}{8}}}{(1-\Gamma_\Omega(\theta))^{\frac{1}{\alpha}-1}}. \quad (6)$$

For a rotation rate $\omega = 0.95$, the variation of the mass loss rate is $\dot{M}({\rm pole}) = 3.25\,\dot{M}({\rm eq})$ (Georgy et al. 2011).

3. Transport processes

In 1D (according to Zahn 1992; Chaboyer & Zahn 1992; Maeder & Zahn 1998) the transport of angular momentum is

$$\rho\frac{\partial}{\partial t}\left(r^2\bar{\Omega}\right)_{M_r} = \cap \frac{1}{5r^2}\frac{\partial}{\partial r}\left(\rho r^4\bar{\Omega}U(r)\right) + \cap \frac{1}{r^2}\frac{\partial}{\partial r}\left(\rho D_{\rm v} r^4\frac{\partial\bar{\Omega}}{\partial r}\right) \quad (7)$$

and the transport of chemical species is

$$\rho\frac{\partial X_i}{\partial t} = \frac{1}{r^2}\frac{\partial}{\partial r}\left(\rho r^2\left(D_{\rm v} + D_{\rm eff}\right)\frac{\partial X_i}{\partial r}\right). \quad (8)$$

In these expressions, $U(r)$ is the radial component of the meridional circulation, $D_{\rm v}$ is the diffusion coefficient due to various mechanisms like convection or shear, and $D_{\rm eff}$ is the diffusion coefficient due to meridional circulation and horizontal turbulence.

The expression for the transport of angular momentum is the full advecto-diffusive expression, but some codes on the market use a diffusion-only approximation to express this transport. When the advective term is taken into account, there exist three different ways to express the horizontal turbulence (Zahn 1992; Maeder 2003; Mathis et al. 2004), and two ways for the shear turbulence (Maeder 1997; Talon & Zahn 1997). A few years ago, Maeder et al. (2013) proposed a global diffusion coefficient taking into account all the various instabilities triggered by rotation (GSF, Solberg-Høiland, thermohaline, ...) and the interplay they have one on each others. The variety of ways to express the mixing process induced by rotation explains the large differences between the outputs of different codes, as highlighted by Chieffi & Limongi (2013).

Note that even without rotation, Martins & Palacios (2013) have shown that large differences exist between the outputs of the various existing codes. One of the main reason for these differences (besides the choice for the opacities, EOS, reaction rates, mass loss recipe, or initial chemical composition and mixture) is the treatment of convection and overshoot. All mixing processes implemented have at least one free parameter modellists need to calibrate on observations, and depending on the choice of the set of data to reproduce, different values can be adopted.

Besides these uncertainties that could be viewed as theoretical error bars, the net effects of rotational mixing are to replenish the core in fresh fuel, hence larger cores, longer lifetimes, higher L. Actually, the behaviour of a star is not monotonic with the increase of rotation. at the beginning of the main sequence, the hydrostatic effects dominate and the star behaves like a lower-mass one. As evolution proceeds, the mixing becomes dominant for low and average rotation, while the rapid rotators keep strong hydrostatic effects. The highest L is therefore observed not in the fastest stars, but in slightly-above-average rotators (see Fig. 1).

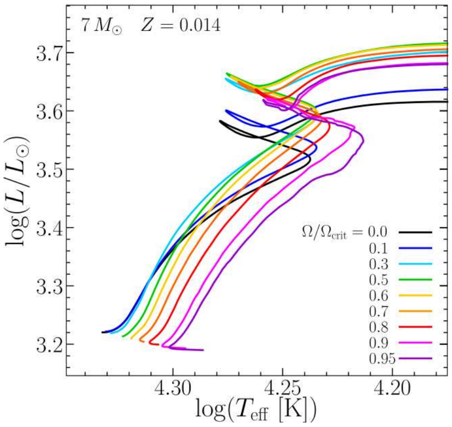

Fig. 1. Main sequence tracks in the Hertzsprung-Russell diagram for models of $7\,M_\odot$ with various initial rotation rates. The models are from Georgy et al. (2013).

The evolution of the surface velocity is governed both by the mass loss (that removes angular momentum from the surface and triggers the meridional currents) and by the internal transport (that generally brings angular momentum from the centre to the surface). The net effect depends on the balance between the two. Massive stars have a strong transport but also strong winds, and generally the surface velocity decreases more or less rapidly during the main sequence. Lower-mass stars have a weaker core-envelope coupling, but also much weaker winds, and their surface velocity remains more or less constant during the main sequence. Note that the surface velocity and its ratio to the critical velocity $V/V_{\rm crit}$ evolve differently: $V_{\rm crit} = \sqrt{\frac{2}{3}\frac{GM}{R_{\rm pol}}}$ decreases always during the main sequence, because the mass decreases and the radius inflates. Therefore, even if the surface velocity decreases with the evolution, the ratio to the critical velocity increases (see Fig. 2).

4. Metallicity effects, multiplicity

The picture depicted above is modulated by various factors, among which the metallicity and the multiplicity status of the stars.

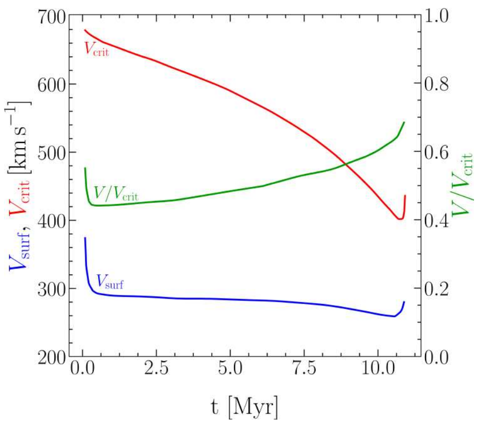

Fig. 2. Model of 18 $M_\odot$ at solar metallicity: main sequence evolution of the surface velocity V (in blue), critical velocity $V_{\rm crit}$ (in red), and ratio $V/V_{\rm crit}$ (in green).

At low metallicity, the winds are weaker, so less angular momentum is removed from the star. The meridional circulation becomes much weaker, which builds a steep Ω-gradient in the interior, inducing a strong shear. The diffusion timescale behaves proportionally to R^2/D; since the stars are more compact, the diffusion time is expected to be shorter. Generally, the surface velocity tends to increase during the main sequence, and the relative enrichment of the surface in heavy elements is larger than at solar metallicity.

When binaries are considered, we have to add some complex ingredients, like tidal forces or mass transfer episodes, that will affect obviously the surface velocity and abundances, but also L and $T_{\rm eff}$. By affecting both the transport of angular momentum and the mass loss experienced by the star, the multiplicity status of a star plays a major role in the evolution of the rotation. However, the complexity of the physics involved makes it extremely difficult to produce reliable models. Some crucial phases, like the phase of common envelope in close binaries, still escapes us, since the true impact on the evolution and the numerical way of implement it is largely still unknown (see Ivanova et al. 2013).

When modelling population synthesis, the huge parameter space needed to be explored makes it impossible to compute grids of binary models at large scales with a detailed physics. Simplifications are mandatory to be able to compute population synthesis (Eldridge et al. 2008). Some codes use a base of single stars models structures and apply to them prescriptions for binary interactions (see for instance de Mink et al. 2013). It is usually considered that the component quickly synchronise and that the rotation rate of the stars are the one of the orbit. However observations show that the real picture might be much more complicated than that (see the results by Martins et al. 2017).

When turning to the predictions of binary models, it is thus important to keep in mind that at best they are tainted by all the uncertainties of single star modelling plus all the uncertainties and unavoidable simplifications of binary interactions modelling.

5. Effects of rotation on clusters

To explore the effects of rotation on the appearance of clusters, we have used the Syclist tool[1] (Georgy et al. 2014). We have generated isochrones at three different ages for various initial rotation rates (see Fig. 3). Generally, the tracks are bluer for a higher rotation rate. Just below the turn-off, the tracks cross each other, and the rotating ones become redder. The turn-off occurs at a higher luminosity when rotation is taken into account. Would one analyse such a cluster with non-rotating isochrones, the age deduced would be younger, because of the higher-L turn-off. The shift in L is due to two effects: first, the increase of the luminosity due to the increase of the core size, as mentioned in Section 3, and second, the longer lifetimes of rotating models, that keeps higher mass stars on the main sequence while the non-rotating ones have already left it. In a M_V-B-V diagram, the effects of rotation are stronger at older ages. The age spread deduced from a population of stars presenting a distribution of rotation rates would increase with the age of the cluster, just

[1] https://www.unige.ch/sciences/astro/evolution/fr/base-de-donnees/syclist/

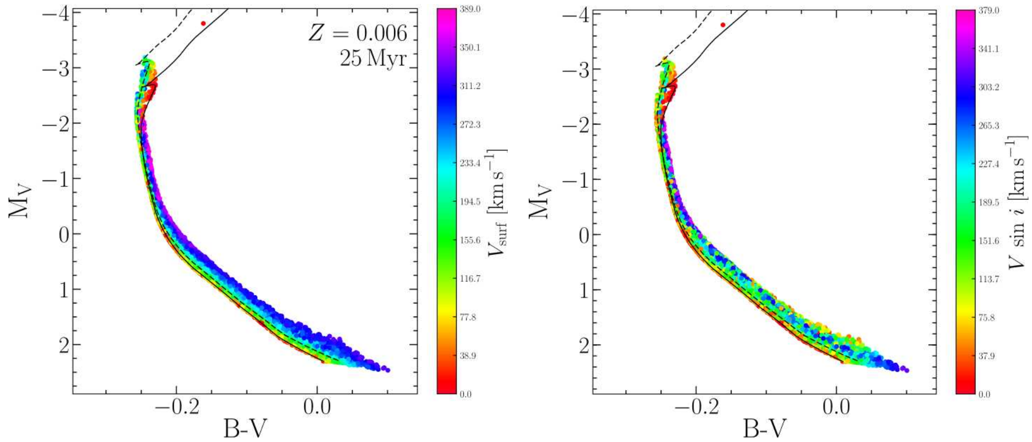

Fig. 4. CMD of a $Z = 0.006$ synthetic cluster of 50'000 stars at 30 Myr, with the initial rotation distribution of Huang et al. (2010). Non-rotating and average-rotation isochrones for this age are also drawn (black solid and dashed lines respectively). Left panel: colour-coded according to the true surface velocity. Right panel: colour-coded according to the 'observed' $V \sin i$.

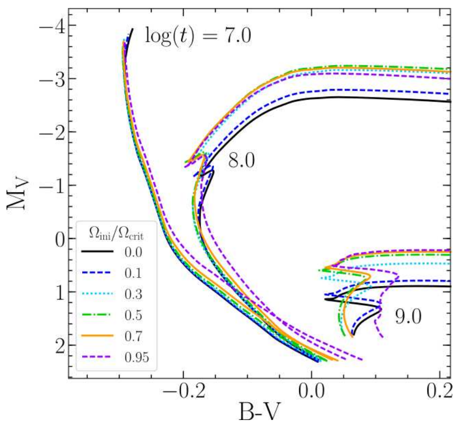

Fig. 3. Isochrones at various ages and for various rotational velocities.

as the observations show it (Niederhofer et al. 2015).

The Syclist tool offers also the possibility to create synthetic clusters, in which we can imprint an initial velocity distribution. The advantage of synthetic clusters is that we can better grasp the variety of stellar populations, and mimic the conditions of observation (angle of view, photometric error, ...). Figure 4 (top panels) shows the result in a CMD colour-coded with $V_{\rm surf}$ (left) and $V \sin(i)$ (right). In these figures, we see that the most rapid rotators ($V \sin(i) > 300\,{\rm km\,s^{-1}}$) are concentrated in the zone where the two isochrones (average-rotating and non-rotating) are crossing. At first sight, besides any angle effect (same feature left and right), it can seem counter-intuitive, since we expect the most rapid rotators to gather at the turn-off. The explanation is simply that the critical velocity decreases rapidly at the end of the main sequence (cf. Fig. 2). While the stars there seem to be average-rotating, they are actually close to the critical velocity, because the latter is lower than it is for the stars in the neck.

The turn-off is widened by the rotation effects, the slowest rotators drawing the dimmer red hook while the rapid rotators drawing the brighter blue hook. In the lower part of the cluster, we expect the slowest rotator to lie close to the non-rotating isochrone, and the most rapid rotators to spread towards the red. However, the angle effect blurs this picture, which is thus not expected to be really observed.

6. Take-home message

The main take-home message of this presentation is that rotation deeply modifies the appearance and evolution of stars. Not taking it into account might drive to false conclusions about the mass and evolutionary status of the star. Rotation shows also a strong metallicity dependance, since Z affects both the mass loss and the strength of the internal mixing. Multiplicity also affects strongly the rotation evolution of stars. The complexity of the physics involved in binaries and the huge parameter space to explore impose drastic simplifications that need yet to be ascertain.

Another point to be cautious about is that there exist large differences between different codes, both due to the basics physics implemented and to the numerical choices made. It is thus delicate to mix models from different grids. Note that these difference could be viewed as theoretical error bars.

Finally, don't forget that theoreticians and observers don't speak the same language. We need to use transformations to go from stellar tracks to observations or vice-versa. The use of stellar population usually helps in bridging the gap.

References

Carciofi, A. C., et al. 2008, ApJ, 676, L41
Chaboyer, B. & Zahn, J.-P. 1992, A&A, 253, 173
Chaboyer, B., Demarque, P., & Pinsonneault, M. H. 1995, ApJ, 441, 865
Chieffi, A. & Limongi, M. 2013, ApJ, 764, 21
de Mink, S. E., et al. 2013, ApJ, 764, 166
Deupree, R. G. 1990, ApJ, 357, 175
Domiciano de Souza, A., Kervella, P., Jankov, S., et al. 2003, A&A, 407, L47
Eddington, A. S. 1925, The Observatory, 48, 73
Eldridge, J. J., Izzard, R. G., & Tout, C. A. 2008, MNRAS, 384, 1109
Endal, A. S. & Sofia, S. 1976, ApJ, 210, 184
Espinosa Lara, F. & Rieutord, M. 2011, A&A, 533, A43
Faulkner, J., Roxburgh, I. W., & Strittmatter, P. A. 1968, ApJ, 151, 203
Fliegner, J. & Langer, N. 1994, in Pulsation, Rotation and Mass Loss in Early-Type Stars, ed. L. A. Balona, H. F. Henrichs, & J. M. Le Contel (Kluwer, Dordrecht), IAU Symp., 162, 147
Georgy, C., et al. 2009, A&A, 502, 611
Georgy, C., Meynet, G., & Maeder, A. 2011, A&A, 527, A52
Georgy, C., Ekström, S., Granada, A., et al. 2013, A&A, 553, A24
Georgy, C., Granada, A., Ekström, S., et al. 2014, A&A, 566, A21
Heger, A. & Langer, N. 2000, ApJ, 544, 1016
Heger, A., Langer, N., & Woosley, S. E. 2000, ApJ, 528, 368
Heger, A., Woosley, S. E., & Spruit, H. C. 2005, ApJ, 626, 350
Huang, W., Gies, D. R., & McSwain, M. V. 2010, ApJ, 722, 605
Ivanova, N., Justham, S., Chen, X., et al. 2013, A&A Rev., 21, 59
Kippenhahn, R. & Thomas, H.-C. 1970, in Stellar Rotation, ed. A. Slettebak (D. reidel, Dordrecht), IAU Coll., 4, 20
Langer, N., et al. 1997, Nucl. Phys. A, 621, 457
Maeder, A. 1997, A&A, 321, 134
Maeder, A. 2003, A&A, 399, 263
Maeder, A. & Zahn, J.-P. 1998, A&A, 334, 1000
Maeder, A. & Meynet, G. 2000, ARA&A, 38, 143
Maeder, A. & Meynet, G. 2001, A&A, 373, 555
Maeder, A., et al. 2013, A&A, 553, A1
Martayan, C., Hubert, A. M., Floquet, M., et al. 2006, A&A, 445, 931
Martins, F. & Palacios, A. 2013, A&A, 560, A16
Martins, F., Mahy, L., & Hervé, A. 2017, ArXiv 1709.00937
Mathis, S., Palacios, A., & Zahn, J.-P. 2004, A&A, 425, 243
Meynet, G. 1996, in From Stars to Galaxies: the Impact of Stellar Physics on Galaxy Evolution, ed. C. Leitherer, U. Fritze-von-Alvensleben, & J. Huchra (ASP, San Francisco), ASP Conf. Ser., 98, 160
Meynet, G. & Maeder, A. 1997, A&A, 321, 465
Meynet, G. & Maeder, A. 2000, A&A, 361, 101
Meynet, G. & Maeder, A. 2003, A&A, 404, 975

Meynet, G. & Maeder, A. 2005, A&A, 429, 581
Monnier, J. D., Zhao, M., Pedretti, E., et al. 2007, Science, 317, 342
Müller, P. E. & Vink, J. S. 2014, A&A, 564, A57
Niederhofer, F., et al. 2015, MNRAS, 453, 2070
Owocki, S. P. & Gayley, K. G. 1997, in Luminous Blue Variables: Massive Stars in Transition, ed. A. Nota & H. Lamers (ASP, San Francisco), ASP Conf. Ser., 120, 121
Petrenz, P. & Puls, J. 2000, A&A, 358, 956
Pinsonneault, M. H., et al. 1989, ApJ, 338, 424
Roxburgh, I. W., Griffith, J. S., & Sweet, P. A. 1965, Zeitschrift fuer Astrophysik, 61, 203
Roxburgh, I. W. & Strittmatter, P. A. 1966, MNRAS, 133, 345
Siess, L. & Livio, M. 1997, ApJ, 490, 785
Talon, S. & Zahn, J.-P. 1997, A&A, 317, 749
Vinicius, M. M. F., Zorec, J., Leister, N. V., & Levenhagen, R. S. 2006, A&A, 446, 643
Vink, J. S. & de Koter, A. 2005, A&A, 442, 587
von Zeipel, H. 1924, MNRAS, 84, 665
Yoon, S., Langer, N., & Norman, C. 2006, A&A, 460, 199
Zahn, J.-P. 1992, A&A, 265, 115
Zhao, M., Monnier, J. D., Pedretti, E., et al. 2009, ApJ, 701, 209